Original Article

Adsorption of Rhodamine B on activated carbon obtained from pericarp of rubber fruit in comparison with the commercial activated carbon

Fareeda Hayeeye*, Maimoon Sattar, Surajit Tekasakul, and Orawan Sirichote

Department of Chemistry, Faculty of Science,
Prince of Songkla University, Hat Yai, Songkhla, 90112 Thailand.

Abstract

Adsorption of the dye, Rhodamine B, on activated carbon obtained from pericarp of rubber fruit (PrAC) was investigated in comparison with the commercial activated carbon (CAC). Both activated carbons were characterized by scanning electron microscopy (SEM), specific surface area, and pH at point of zero charge (pH_{pzc}). The effects of various experimental parameters such as contact time, dye concentration, amount of activated carbon, pH and temperature were analysed. The adsorption isotherm fitted well into the Langmuir model. By keeping pH constant at 4.0 and varying temperatures at 30, 40, 50, and 60°C, the maximum adsorption were 0.2306, 0.2356, 0.2756, and 0.2981 mmol g^{-1} for PrAC and 0.8957, 0.9588, 0.9841, and 1.0263 mmol g^{-1} for CAC, respectively. Study of the effect of temperature dependence of these adsorptions indicated that they were endothermic processes. The adsorption efficiency of Rhodamine B on PrAC is about 80-90%.

Keywords: activated carbon, pericarp of rubber fruit, Rhodamine B, Langmuir adsorption isotherm

1. Introduction

Waste water including waste water from manufacturing processes, buildings, residences, and shops may contain substances such as organic substances, inorganic substances, acid alkaline, heavy metals, some chemical substances, radioactivity substances, toxic substances, sandy soil, and other wastes. When these wastes are expelled into the river, the quantity of those substances may be toxic is living things in the water. Most of the contaminants in waste water from the dye industry are dyes and chemical substances which are left over part in the water using in manufacturing process and being thrown into the waste water. Even in low concentrations, dyes affect aquatic life and the food web. Because many organic dyes are harmful to human beings, the removal of color from the waste effluents is environmentally important (Arivoli *et al.*, 2009).

There are many communities in various provinces of the lower part of southern Thailand that produce Krajood products or products made from Bulrush plant such as mats, bags, hats and shopping baskets. The dying of raw materials in different colors is needed to increase the variety and improve the quality of the products. Rhodamine B, which is a dark pink basic dye, was exclusively used for many patterns of Krajood products. In this research the Rhodamine B was selected for the adsorption experiment due to its presence in the wastewater of several industries (such as textile, leather, jute and food industries). Its structure in aqueous solution is displayed in Figure 1. There are many methods to remove the color but one of the interesting ways is adsorption by activated carbon. Activated carbon is the most widely used adsorbent for this purpose because of its extensive surface area, microporous structure, high adsorption capacity, and high degree of surface reactivity (Bhatnagar *et al.*, 2005).

In the present work the activated carbon obtained from pericarp of rubber fruit (PrAC) were used to study the adsorption of Rhodamine B in comparison with commercial activated carbon (CAC). The pericarp of rubber fruit (PrAC)

---

* Corresponding author.
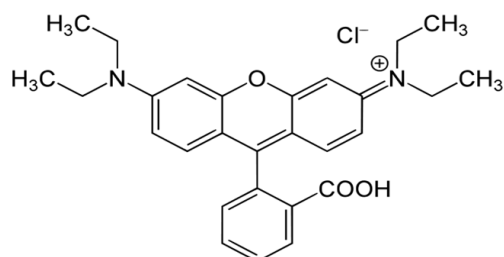 Email address: hin_999@hotmail.com

Figure 1.   Structure of Rhodamine B in aqueous solution.

was used obtained from the rubber plantation and used of prepare activated carbon using chemical activation with $ZnCl_2$.

The chemical activation is considered of a suitable method for producing highly microporous activated carbons. The most common activating agent is zinc chloride ($ZnCl_2$). In comparison with the physical activation, the chemical activation mechanism is not well understood (Lozano-Castello *et al.*, 2001) but it seems that the chemical agent dehydrates the sample, inhibits the tar formation and volatile compound evolution, and therefore enhances the yield of the carbonization process (Williams and Reed, 2004). After impregnating the precursor by chemical agent and heat treatment of the mixture, the impregnating agent is eliminated by washing with acid/base and water. The washing step makes the pore structure available, by removing the impregnating agent and its salts. Figure 2 shows the general flow chart for chemical activation by zinc chloride ($ZnCl_2$). The activated carbon produced by $ZnCl_2$ activation is dominantly microporous, but with a significant component of mesopores which increases with an increase in the impregnation ratio ($ZnCl_2$/precursor) (McEnanney, 2002; Azargohar, 2009).

2. Materials and Methods

2.1 Materials and reagents

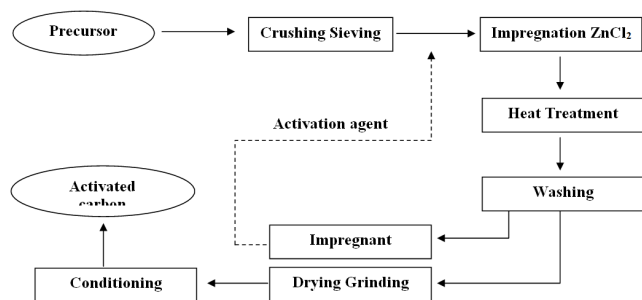Rhodamine B was procured from Fluka, UK. The CAC was obtained from Sigma – Aldrich, UK. The production

Figure 2.   The general flow chart for chemical activation by zinc chloride ($ZnCl_2$).

processes of activated carbon from pericarp of rubber fruit were carbonization and chemical activation with $ZnCl_2$. Pericarp of rubber fruit was dried in the sun and cut into small pieces approximately 1 inch and placed into a stainless steel box with cover. The carbonization was then conducted in a muffle furnace at 400°C for 1 h. After carbonization the residual char was ground in a laboratory jar mill to pass throughs 200-270 mesh sieves. Then, the chemical activation was performed by mixing the ground char with concentrated solution of $ZnCl_2$ at a ratio of 1:2. The sample was activated at 600°C for 3 h in the muffle furnace. The obtained activated carbon was washed with 1% HCl solution. In the next step, the carbon was soaked in hot water for five minutes and subsequently the water was drained off through a Buchner funnel. This step was repeated two more times to obtain a neutral pH value. Finally, it was dried in the oven at 110°C for 24 h. The obtained activated carbon was kept in a dessicator (Chuenchom, 2004; Sirichote *et al.*, 2008).

2.2 Characterization of the activated carbons

A scanning electron microscope (JSM-5800 LV) at the Scientific Equipment Center, PSU, was used to analyze the porosity of both activated carbon samples.

Nitrogen adsorption isotherms at 77 K (Coulter SA 3100) were used to determine specific surface area and micropore volumes of activated carbons by using Brunauer-Emmett-Teller (BET) and t-plot equations, respectively. The pore size distribution was calculated by using the Barrett-Joyner-Halenda (BJH) model. Prior to the adsorption experiments, for maintaining the integrity of the chemical surface properties, all samples were degassed for 1 h at 120°C.

The pH_{pzc} was determined by using the pH drift method (Jia *et al.*, 1998; Jia *et al.*, 2002) for all activated carbon samples. The pH of solution of 0.1 M NaCl was adjusted between 2-12 by using 0.01 M HCl or NaOH. Activated carbon sample (0.6000 g) was added into 100 mL of NaCl solution in a 250 mL flask. The flask was sealed to eliminate any contact with air and then left at ambient temperature. The final pH was recorded after the pH had stabilized (typically after 24 h). The graph of final pH (pH_f) versus initial pH (pH_0) was used to determine the point at which initial pH and final pH of activated carbon solution were equal. At this point, (pH_{pzc}), the surface of activated carbon is neutral.

2.3 Adsorption studies

1000 mg L^{-1} stock solution of Rhodamine B was prepared by dissolving in distilled water. Then the stock solution was diluted with distilled water to obtain series of standard solutions with concentrations ranging from 150-500 mg L^{-1}.

The effects from other variable parameters such as the amount of activated carbon, contact time, pH and temperature were also studied.

The various doses of the activated carbons in the range $0.0500 - 0.1000$ g for PrAC and $0.01000 - 0.03500$ g for CAC were mixed with 50 mL of the dye solutions and the mixtures were agitated in a mechanical thermostat shaker at 30°C. The adsorption capacities of activated carbons for different doses were determined at definite time intervals by keeping pH at 4, initial concentration of dye 300 mg L^{-1} and temperature at 30°C.

The effect of contact time on the adsorption of dye by the adsorbent in a single cycle was determined by keeping pH at 4, initial concentration 300 mg L^{-1}, the amount of activated carbon 0.0900 g for PrAC and 0.0200 g for CAC and temperature at 30°C.

The pH of Rhodamine B solution of 300 mg L^{-1} was adjusted between 2 - 13 using 0.01 M HCl or 0.01 M NaOH. A certain amount of activated carbon was added into 50 mL of dye solution. The contents were then shaken at 30°C in the thermostat shaker water bath. After the equilibriums were obtained (24 h for PrAC and 6 h for CAC) about 2 mL of dye solution was transferred to test tube and centrifuged. The supernatant was decanted and analyzed for the concentration of Rhodamine B. The parameters like dosage of the adsorbents (0.0900 g of PrAC and 0.0200 g of CAC), dye concentration (300 mg L^{-1}) and temperature (30°C) were kept constant.

The adsorption experiments were performed at 30, 40, 50 and 60°C in a thermostated water bath shaker at pH 4.0, which is the natural pH of dye solution, to determine the effect of temperature for adsorption. All other factors were kept constant as mentioned above.

2.3.1 Adsorption isotherm studies of Rhodamine B on activated carbons

A certain amount of activated carbon (0.0900 g of PrAC and 0.0200 g of CAC) was added into 50 mL of dye solution. Adsorption equilibrium studies of Rhodamine B on either PrAC or CAC were carried out in a batch process at 30, 40, 50 and 60°C. The concentrations of dye solutions at pH 4.0 were varied in the range of 150 - 400 mg L^{-1}. The contents were centrifuged after gentle shaking for a period of time to reach equilibrium. Rhodamine B concentrations before and after adsorption were then determined by UV-Vis spectrophotometer at a wavelength 554 nm. The adsorbed amount of Rhodamine B was calculated from the equation (1) (Meikap et al., 2006) as follows:

$$Q_e = \frac{V(C_0 - C_e)}{W} \qquad (1)$$

where Q_e is the amount of dye adsorbed onto activated carbon (mg g^{-1}), V is the volume of the solution (L), C_0 is the initial liquid-phase concentration of dye (mg L^{-1}), C_e is the equilibrium liquid-phase concentration of dye (mg L^{-1}), and W is the mass of the adsorbent (g). The amount of dye adsorbed onto activated carbon was calculated based on the previously determined calibration curve.

3. Results and Discussion

3.1 Characterization of PrAC and CAC

3.1.1 Scanning electron microscopy (SEM)

In Figure 3, the scanning electron micrographs of the external structures of both activated carbons, PrAC 200–270 mesh and CAC 200–270 mesh are shown. From micrographs, it can be seen that both samples are full of holes with diameters ranging from around 7.5–10.5 μm and 4-20 μm, respectively. These holes are defined as macropore of the activated carbon (>50 nm). Both micropore and mesopore are not resolved by scanning electron microscopy even at higher magnification because of the limit of detection of the instrument.

3.1.2 Surface area

Nitrogen adsorption isotherms measured for PrAC and CAC are shown in Figure 4. It is evident that the isotherms can be classified into two types.

In the case of PrAC, its isotherm is approximately type I according to IUPAC classification (Hu and Vansant, 1995) since most of the adsorbed volume is contained in the micropores. The isotherms show a steep rise of the initial part where micropores are filled by nitrogen molecule completely at ~0.2 P_s/P_0. After 0.2 P_s/P_0, the isotherm becomes a plateau. It is now widely accepted that the initial part of the type I isotherm represented micropore filling and that the slope of the plateau at high relative pressure is due to monolayer adsorption on the nonmicroporous structures, such as in mesopores, in macropores, and on the external surface.

If nitrogen adsorption isotherm of any porous material can be fitted with type I isotherm, it can be assumed that the material has significant micropores. Thereby, PrAC has the contents largely of micropore. On the other hand, isotherm of CAC belongs to a mixed type in the IUPAC classification (Juang *et al.*, 2002). In the initial parts it is type I, with an important uptake at low relative pressures. It is type II at intermediate and high relative pressures. The steep rise of
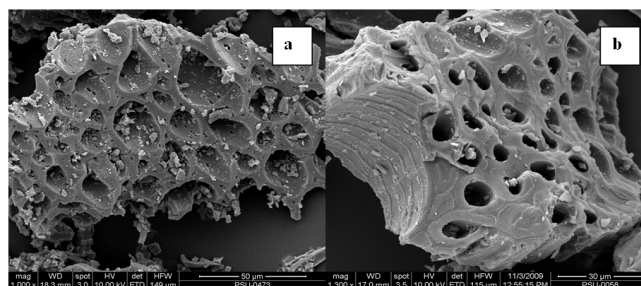

Figure 3. SEM micrographs of (a) PrAC - 200-270 (×1000 magnification) and (b) CAC - 200-270 (×1300 magnification).
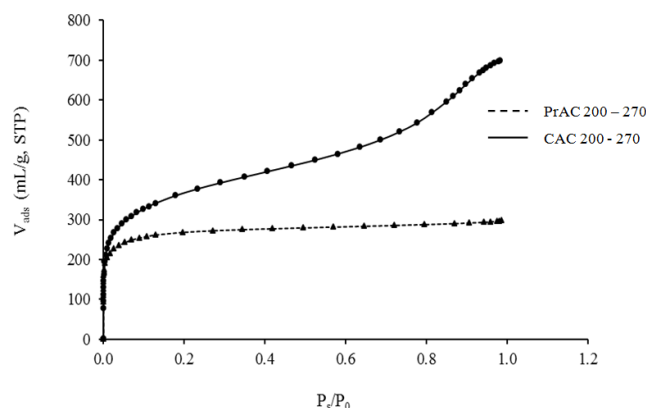
Figure 4. Adsorption isotherms of N_2 at 77 K for the PrAC and CAC (P_s/P_0 is relative pressure).

the initial part of the isotherms evidences the presence of micropores. However, the present samples do not reach a clear plateau unlike other activated carbons. This indicated that PrAC and CAC are mainly micro- and mesoporous in character with a minor presence of wider pores where capillary condensation occurred.

From Table 1, further understanding of the porous characters of the two samples of activated carbon can be obtained. The results show that each sample possesses a well-developed porous structure. PrAC and CAC exhibit different BET surface areas. The difference among BET surface area of the two samples is about 30%. Hence, BET surface area may affect the adsorption efficiency in this study. Generally, the pores of activated carbon are classified into three groups, micropore (< 2 nm), mesopore (2-50 nm) and macropore (> 50 nm). In this study, however, pore size distribution in the micropore region cannot be measured due to the limitation of the instrument. There are many methods for determinations of pore size distribution in the micropore region such as the potential theory of Dubinin, t-plot method, α plot or MP methods (Strelko and Malik, 2002), which are widely used for micropore evalution. This research has used t-plot method for determining micropore surface area, micropore fraction and micropore volume but this method cannot be used for determination of the distribution of micro porous. Pore size distribution above 2 nm, however, can be assessed accurately using the method of Barrett, Joyner and Halenda (BJH) model (Barrett *et al.*, 1951).

It can be seen from Table 1 that PrAC possesses greater micropore surface area and percentage of micropore fraction ((micropore surface area/ BET surface area) ×100) around 75% which is more dues the CAC. Noticeably, CAC has more BET surface area than PrAC but CAC shows less micropore fraction. From Figure 4, CAC remarkably has more incremental pore volume of mesopore and macropore than PrAC. Therefore, the physical characteristics of raw material seem to be important factor for porous nature of activated carbon.

Figure 5 shows the meso- and macropore nature of all activated carbon. PrAC does not have significant mesopores and macropores In contrast, CAC possesses a significant amount of mesopore with a maximum at 6 nm and 16 nm. PrAC also shows evidence of the presence of mesopores and macropores.

3.1.3 Point of zero charge (pH$_{pzc}$)

Graphs of final pH versus initial pH obtained by using the pH drift method for all activated carbon samples are plotted as shown in Figure 6. The results show that pH$_{pzc}$ of PrAC and CAC are 6.5 and 3.5, respectively. It is suggested that the surface of the PrAC in dye solution at pH 4.0 (<pH$_{pzc}$) has positive charge which causes the electrostatic repulsion with the positive charge of the dye. In contrast to the surface of CAC in dye solution at pH 4.0 (>pH$_{pzc}$) has negative charge that can attract with the positive charge of the dye.
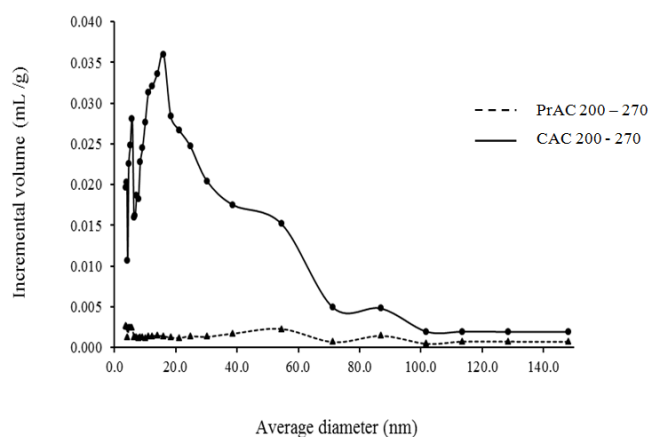

Figure 5. BJH pore size distribution of PrAC and CAC.

Table 1. BET and micropore surface areas of PrAC and CAC

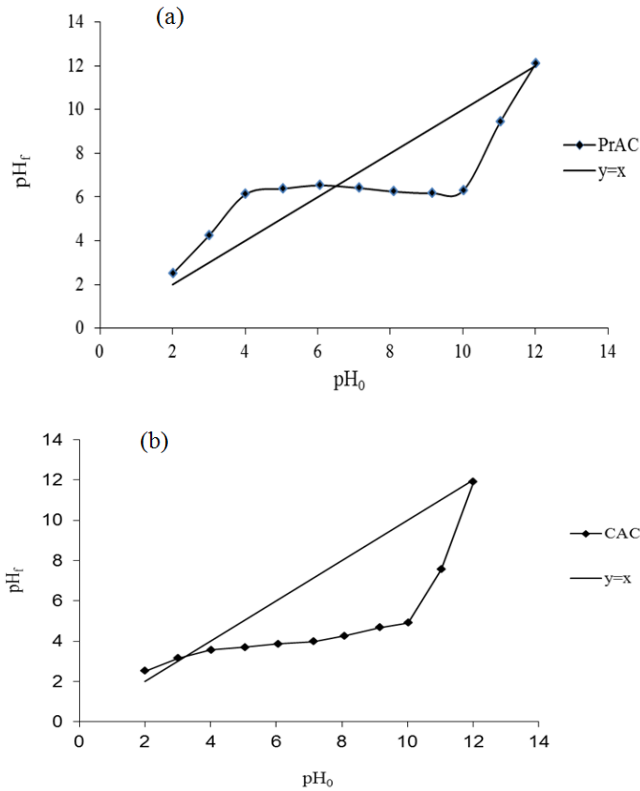| Sample	BET surface area ($m^2 g^{-1}$)	Micropore surface area ($m^2 g^{-1}$)	Micropore fraction (%)	Micropore volume ($mL g^{-1}$)
PrAC	920.69	698.26	75.84	0.32
CAC	1,316.90	492.40	37.39	0.20

Figure 6. Graphs of final pH versus initial pH for determination the point of zero charge (pH_{pzc}) of PrAC 200-270 (a) and CAC 200-270 (b).

The amphoteric character of surface oxides S-CO₂ where S represents the activated carbon surface can be explained as follows (Kadirvalu *et al.*, 2000).
For pH < pH_{pzc}, the dominant reaction is:

$$S - CO_2 + 2H_2O \leftrightarrow S - C(OH^+)_2 + 2OH^-$$
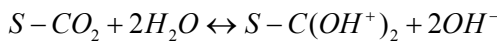
The release of hydroxyl ions induces an increase of pH and a protonated surface of activated carbon.
For pH > pH_{pzc}, the following reaction takes place:

$$S - CO_2 + 2H_2O \leftrightarrow S - C(O^-)_2 + 2H_3O^+$$
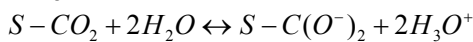
The activated carbon surface is deprotonated and the release of protons induces a decrease in pH.

3.2 Adsorption studies

3.2.1 Effect of various parameters

1) Weight of activated carbon

By keeping the initial concentration at 300 mg L⁻¹ the percentage of dye adsorption at equilibrium increased with increasing weight of both activated carbons as shown in Figure 7. Effect of weight of activated carbon was attributed to the increase of surface area and availability of more adsorption sites (Namasivayam *et al.*, 1996; Navasivayam

and Kadirvelu, 1999). In this study, the appropriate weights of CAC and PrAC were 0.0200 and 0.0900, respectively because these weights of adsorbent did not help too long a time to reach equilibrium for adsorption of Rhodamine B. These fined amounts of activated carbon dose were picking up to study the adsorption isotherm.

2) Contact time and initial dye concentration

In most adsorption isotherm studies, the results showed that equilibrium was achieved within around 24 h and 6 h for PrAC and CAC as shown in Figure 8 by keeping the pH at 4, initial concentration 300 mg L⁻¹, with weight of PrAC and CAC of 0.0900 g and 0.0200 g, respectively, and temperature at 30°C. However, the solutions were left longer than equilibrium time to ensure complete equilibration which were uses of to study the adsorption isotherms.

3) pH

In Figure 9, it shows the effect of solution pH values on the adsorption of Rhodamine B on all of the activated
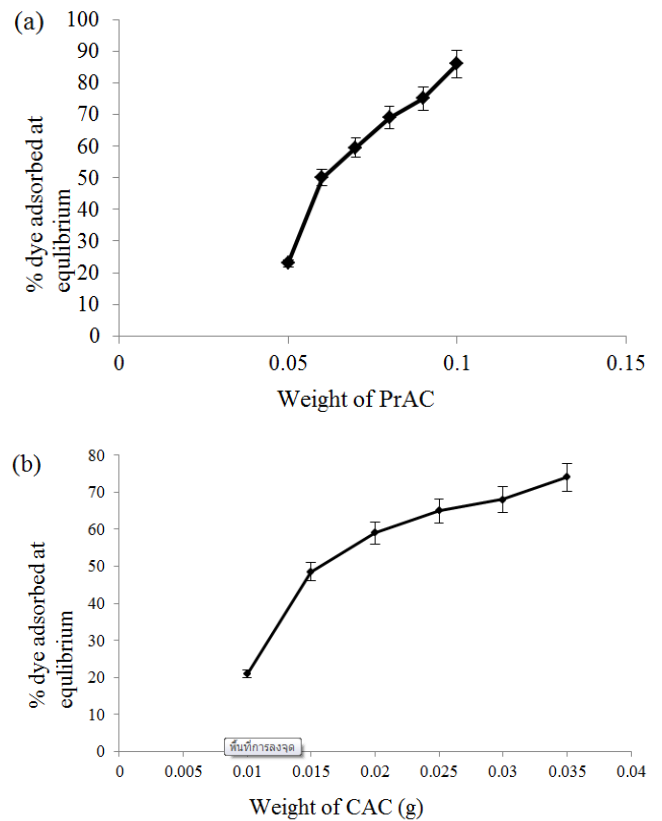

Figure 7. Effect of weight of PrAC (200-270 mesh), 0.0500-0.1000 g/50 mL (a) and effect of weight of CAC (200-270 mesh), 0.0100-0.03500 g/50 mL (b) for adsorption of dye to reach the equilibrium at 30°C, pH = 4.0 and dye concentration 300 mg L⁻¹.
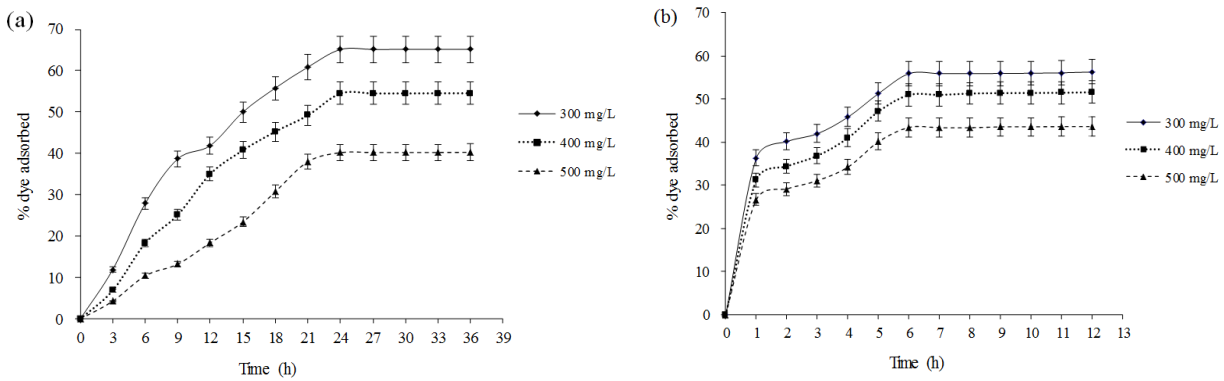
(a)

(b)

Figure 8. Equilibrium time of 300, 400 and 500 mg L^{-1} Rhodamine B on PrAC (0.0900 g) (a) and CAC (0.0200 g) (b) at 30°C and pH = 4.0.
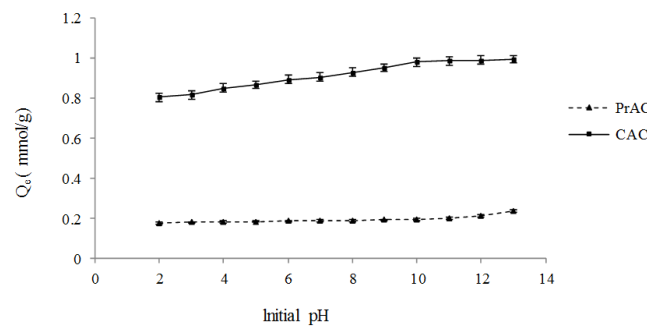
Figure 9. Adsorption of Rhodamine B on PrAC and CAC with pH range 2-13 and dye concentration 300 mg L^{-1}.

carbons. Rhodamine B displays a general trend of slightly increased adsorption on each the activated carbons with the increase of solution pH values.

At pH higher than 2, the adsorption amount of Rhodamine B on PrAC and CAC slightly increased with the increase of solution pH values. In addition, at low pH there was competition for the surface sited of activated carbon between protonation (H^{+} adsorption on the carbon surface) and adsorption of Rhodamine B.

Since the surface of CAC and PrAC are negative at pH > pH$_{pzc}$ (3.5) and pH > pH$_{pzc}$ (6.5), respectively. When pH of solution increases with increasing amount of adsorbed because the increase of solution pH values, the electrical repulsion force become weaker and the Rhodamine B may be transported to the surface of the activated carbons and become to attached on the surface due to the action of other factors such as less competitive from protonation.

4) Temperature

The adsorption capacity of the adsorbent increased with increase in the temperature of the system from 30-60°C as shown in Table 2 and 3 for PrAC and CAC, respectively. The percentage of adsorption increases with increasing temperature. This indicates that the adsorption proces s is endothermic. This result is related with thermodynamic study.

3.3 Adsorption isotherm studies of Rhodamine B on activated carbons

The experimental data were analyzed by the linear form of the Langmuir isotherms (Langmuir, 1918). The Langmuir isotherm was represented by the following equation (2):

$$\frac{C_e}{Q_e} = \frac{1}{Q_m b} + \frac{C_e}{Q_m} \tag{2}$$

where C_e is the equilibrium concentration (mmol L^{-1}), Q_e is the amount adsorbed at equilibrium (mmol L^{-1}) and Q_m and b are Langmuir constants related to the maximum adsorption at monolayer coverage (mmol g^{-1}) and the adsorption equilibrium constant (L mmol^{-1}), respectively.

According to the Langmuir equation the equilibrium concentration of dye over the adsorbed amounts of dye (C_e / Q_e, g L^{-1}) were plotted against the equilibrium concentrations of dye (C_e) at various temperatures for PrAC and CAC as shown in Figure 10. For each temperature the graph was fitted to a straight line. Then the maximum amount of dye adsorption, Q_m (mmol g^{-1}), was calculated from the slope (= $1/Q_m$) and the equilibrium constant related to the heat of adsorption, b (Lmmol^{-1}), was calculated from the intercept (= $1/(bQ_m)$). The values of Q_m and b including the correlation coefficients, R^2, are tabulated in Table 4.

Table 2. Equilibrium parameters for the adsorption of Rhodamine B
0.3000–0.8000 mmol L^{-1} on PrAC

C_0 (mmol L^{-1})	C_e (mmol L^{-1})				% dye adsorbed			
	Temperature (°C)							
	30	40	50	60	30	40	50	60
0.3000	0.0655	0.0568	0.0295	0.0273	78	82	90	91
0.4000	0.1043	0.0907	0.0756	0.0633	75	78	82	85
0.5000	0.1619	0.1504	0.1216	0.1065	69	71	77	79
0.6000	0.2411	0.2274	0.1835	0.1432	61	64	71	77
0.7000	0.3576	0.3526	0.2864	0.2080	51	52	61	72
0.8000	0.4512	0.4332	0.3699	0.3476	46	48	56	58

Table 3. Equilibrium parameters for the adsorption of Rhodamine B
0.3000 – 0.8000 mmol L^{-1} on CAC

C_0 (mmol L^{-1})	(mmol L^{-1})				% dye adsorbed			
	Temperature (°C)							
	30	40	50	60	30	40	50	60
0.3000	0.0954	0.0885	0.0806	0.0619	68	72	74	80
0.4000	0.1271	0.1180	0.1137	0.0979	68	71	73	76
0.5000	0.2113	0.1785	0.1734	0.1705	58	66	67	67
0.6000	0.2952	0.2828	0.2684	0.2562	53	55	57	59
0.7000	0.3957	0.3742	0.3735	0.3612	46	49	49	50
0.8000	0.5125	0.4893	0.4757	0.4505	39	41	43	46

Figure 10 show that adsorption capacities of CAC for Rhodamine B are greater than PrAC at pH = 4 and 30°C, 40°C, 50°C, and 60°C. We can imagine that in the case of the high ionic radius of Rhodamine B, the result may be explained in terms of pore accessibility (Kadirvalu *et al.*, 2000). Since PrAC has more micropores than CAC, some micropore entrances may be blocked by hydrolyzed dye species which are larger than the dye ions. Accordingly, surface groups located in micropores are no longer accessible and some surface sites are not used for adsorption. In the case of CAC which contain more mesopores, accessibility to micro- and mesopores is not blocked by hydrolyzed species and almost all surface sites can be used for adsorption of Rhodamine B. In addition, acidity of the surface becomes another factor to define adsorption capacities (Ferro-Garcy *et al.*, 1998). CAC, which has lower pHpzc values, should have more adsorption capacities than PrAC. Therefore, it is unequivocal that the CAC has higher adsorption of Rhodamine B than PrAC because CAC has the higher mesopore and lower pHpzc value.

The dimensionless separation factor (R_L) is used to confirm the favorability of the adsorption process, which is calculated by the following equation (3) (Arivoli and Thenkuzhali, 2007):
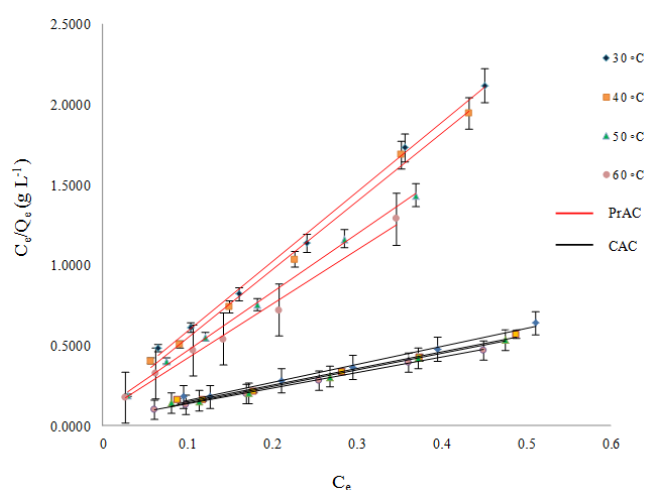
Figure 10. Langmuir adsorption isotherms for linear form of Rhodamine B on PrAC and CAC at 30°C, 40°C, 50°C and 60°C, dye concentrations 150-400 mg L^{-1} and pH = 4.0.

$$R_L = \frac{1}{1 + bC_0} \tag{3}$$

Table 4. Parameter values of the Langmuir equations for linear form fitted to the experiment of Rhodamine B adsorption on PrAC and CAC at different temperatures

Temp (°C)	PrAC			CAC		
	Q_m (mmol g^{-1})	b	R^2 (L mmol^{-1})	Q_m (mmol g^{-1})	b (L mmol^{-1})	R^2
30	0.2306	29.0818	0.9964	0.8957	24.7013	0.9908
40	0.2356	34.5570	0.9953	0.9588	24.9522	0.9903
50	0.2756	35.1872	0.9982	0.9841	25.9898	0.9944
60	0.2981	40.5671	0.9902	1.0263	29.7073	0.9988

Where R_L is its dimensionless separation factor, b is an equilibrium constant related to the heat of adsorption and C_0 is the initial dye concentration. The R_L values were found between 0 and 1 confirming that the ongoing adsorption process was favorable. Their values are presented in Table 5 and Table 6 for PrAC and CAC, respectively.

3.4 Thermodynamic considerations

From the previous study, some general conclusions can be drawn regarding the energetic changes occurring

Table 5. Dimensionless separation factor (R_L) of Rhodamine B adsorption on PrAC at different temperature

C_o (mg L^{-1})	R_L Temperature(°C)			
	30	40	50	60
150	0.0994	0.0850	0.0836	0.0733
200	0.0766	0.0653	0.0642	0.0561
250	0.0622	0.0529	0.0520	0.0454
300	0.0523	0.0444	0.0436	0.0380
350	0.0450	0.0381	0.0375	0.0327
400	0.0396	0.0335	0.0329	0.0287

Table 6. Dimensionless separation factor (RL) of Rhodamine B adsorption on CAC at different temperature

C_o (mg L^{-1})	R_L Temperature(°C)			
	30	40	50	60
150	0.1148	0.1140	0.1099	0.0975
200	0.0888	0.0882	0.0849	0.0751
250	0.0723	0.0718	0.0691	0.0610
300	0.0609	0.0604	0.0582	0.0512
350	0.0524	0.0521	0.0501	0.0441
400	0.0462	0.0458	0.0441	0.0388

during the process. The b parameter from Langmuir equation can be related to the enthalpy or heat of adsorption (ΔH_{ads}) as follows (Adamson and Gast, 1997)

$$b = b'e^{(-\Delta H_{ads}/RT)} \qquad (4)$$

where R is the universal gas constant (8.314 J K^{-1} mol^{-1}), T is the temperature in Kelvin and b' is a pre-exponential factor constant. The heat of the adsorption (ΔH_{ads}) can be determined from its slope of the observed linearity from the van't hoff plot of ln b versus 1/T that leads to the heat process involved in adsorption at monolayer coverage on PrAC and CAC The values of heat adsorption (ΔH_{ads}) were 9.4939 kJ mol^{-1} and 4.8660 kJ mol^{-1} for PrAC and CAC, respectively, and the results are shown in Figure 11. There is another alternative use the Clausius-Clapeyron equation to explain heat of adsorption.

The heat of adsorption was calculated by applying the Clausius-Clapeyron equation to the adsorption isotherm as following equation (Alberty and Silbey, 1992; Sirichote, 2002):

$$\frac{dP}{dT} = \frac{P\Delta H_{vap}}{RT^2} \qquad (5)$$

where P is the equilibrium pressure of gas, T is the absolute temperature, ΔH_{vap} is the heat of vaporization, and R is the gas constant. On rearrangement equation (5) becomes
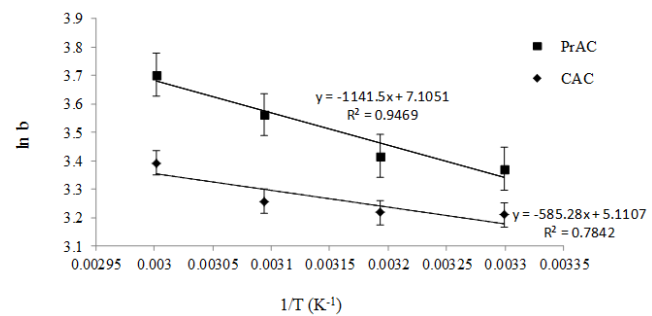

Figure 11. The van't hoff plots for adsorption of Rhodamine B on PrAC and CAC at 30°C, 40°C, 50°C and 60°C, dye concentrations 150-400 mg L^{-1} and pH = 4.0.

$$\frac{dP}{P} = \frac{\Delta H_{vap}}{RT^2} dT \qquad (6)$$

$$d \ln \frac{P}{P^0} = \frac{\Delta H_{vap}}{RT^2} dT \qquad (7)$$

where P^0 is the standard pressure used.

Replacement of P by CRT and P^0 by C^0RT from ideal gas law where C is the molar concentration and C^0 is the standard value of the molar concentration (1 mol L^{-1}) equation (7) becomes

$$d \ln \frac{C}{C^0} = \frac{\Delta H_{vap}}{RT^2} dT \qquad (8)$$

For adsorption in solution the ΔH_{vap} is replaced by ΔH_{ads} which is the heat of adsorption. Integrating on the assumption that the ΔH_{ads} is independent of temperature and concentration and since the term ln C^0 is equal to zero, equation (8) yields

$$\int_{C^\circ}^{C_e} d \ln C = \frac{\Delta H_{ads}}{R} \int T^2 dT \qquad (9)$$

$$\ln C_e = -\frac{\Delta H_{ads}}{RT} + c \qquad (10)$$

where C_e is the equilibrium concentration (mmol L^{-1}), ΔH_{ads} is the isosteric heat of adsorption (kJ mol^{-1}), R is the universal gas constant (8.314 J K^{-1} mol^{-1}), and c is the integration constant. The plots of applied Clausius-Clapeyron equation to adsorption isotherm in equation (10) as ln C_e versus $1/T$ should give a straight line of slope -($\Delta H_{ads}/R$) and the results are shown in Figure 12(a) and Figure 12(b). The values of the heat of adsorption (ΔH_{ads}) are shown in Table 7

The positive values of the heat of adsorption (ΔH_{ads}) from van't hoft equation and Clausius-Clapeyron equation
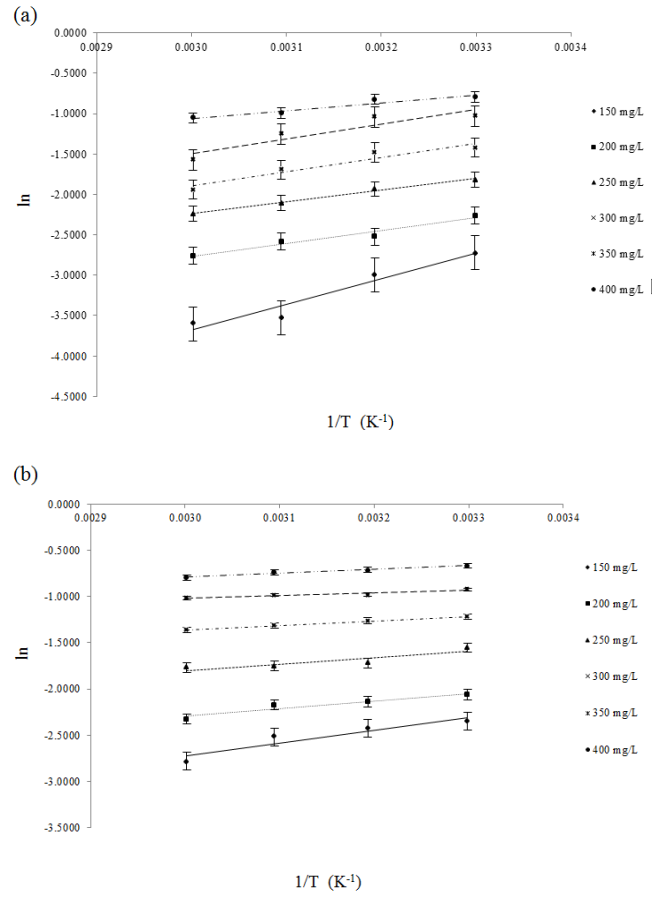

Figure 12. Clausius-Clapeyron plots for adsorption of Rhodamine B on PrAC and CAC at 30°C, 40°C, 50°C and 60°C, dye concentrations 150-400 mg L^{-1} and pH = 4.0.

indicated that they were endothermic processes and the ΔH_{ads} of between 0–40 kJ mol^{-1} confirms that it governs the possibility of physical adsorption (Bond, 1987).

Table 7. The heat of adsorption (ΔH_{ads}) of Rhodamine B adsorption on PrAC and CAC from Clausius-Clapeyron equation at 30°C, 40°C, 50°C and 60°C, 150–400 mg L^{-1} and pH = 4.0

C_0 (mg L^{-1})	PrAC		CAC	
	ΔH_{ads} (kJ mol^{-1})	R^2	ΔH_{ads} (kJ mol^{-1})	R^2
150	27.56±0.05	0.9001	11.58±0.05	0.8895
200	14.08±0.05	0.9931	6.84±0.05	0.9179
250	12.30±0.05	0.9648	5.71±0.05	0.7951
300	14.81±0.05	0.9286	4.01±0.03	0.997
350	15.23±0.03	0.8574	2.32±0.03	0.894
400	7.88±0.02	0.9451	3.48±0.02	0.984
Average value of ΔH_{ads}	15.31		5.67	

4. Conclusions

The characteristics of adsorption of Rhodamine B on PrAC and CAC can be correlated reasonably well by the Langmuir adsorption isotherm. By keeping pH 4.0 and varying temperatures at 30, 40, 50 and 60°C, the maximum adsorption (Q_m) were 0.2306, 0.2356, 0.2756 and 0.2981 mmol g^{-1} for PrAC and 0.8957, 0.9588, 0.9841 and 1.0263 mmol g^{-1} for CAC, respectively. The values of maximum adsorption (Q_m) for CAC are greater than for PrAC, showing the importance of porosity, pore size for adsorption and the charge on the surface of activated carbon. CAC has a significantly larger amount of mesopores and macropores than PrAC, indicating that the adsorption of dye occurs in mesopores and macropores of CAC. The pH of dye solution at 4.0 causes the surface of CAC to have negative charges which will attract the positively charged dye. In contrast, the surface of PrAC with positive charges causes electrostatic repulsion of the dye. However, the aromatic rings of dye molecule can be attract of weakly to the neutral part of PrAC surface by van der Waals interaction. The R_L values are found to in the range between 0 and 1, which confirms that the ongoing adsorption process is much more favorable. The average values of heat adsorption (ΔH_{ads}) were 15.31 kJ mol^{-1} and 5.67 kJ mol^{-1} for PrAC and CAC, respectively. These ΔH_{ads} are between 0–40 kJ mol^{-1} confirm the adsorption processes to be endothermic and controlling the physical adsorption. The efficiency of adsorption of Rhodamine B on PrAC is about 80-90%. Therefore, one of the agricultural products like PrAC can replace the commercial activated carbon for removal of dyes from waste water.

Acknowledgments

References

Adamson, A. W. and Gast, A. P. 1997. Physical Chemistry of Surfaces, John Wiley and Sons Canada, Ltd., Canada, pp. 521-523.

Alberty, R.A. and Silbey, R. J. 1992. Physical Chemistry (1st ed.), John Wiley and Sons, Inc., New York, U.S.A., p. 187.

Arivoli, S. and Thenkuzhali, M. 2007. Kinetic, mechanistic, thermodynamic and equilibrium studies on the adsorption of Rhodamine B by acid activated low cost carbon. E-Journal of Chemistry. 5, 187-200.

Arivoli, S., Thenkuzhali, M.; and Martin Deva Prasath, P. 2009. Adsorption of Rhodamine B by acid activated carbon – kinetic, thermodynamic and equilibrium Studies. E-Journal of Chemistry. 1(2), 138-155.

Azargohar, R. 2009. Production of activated carbon and its catalytic application for oxidation of hydrogen sulphide. Doctor of Philosophy in the department of Chemical Engineering University of Saskatchewan. Canada.

Barrett, E. P., Joyner, L. G. and Halenda, P. P. 1951. Pore size distribution for porous materials. Journal of the American Chemical Society. 73, 373-380.

Bhatnagar, A. and Jain, A.K. 2005. A comparative adsorption study with different industrial wastes as adsorbents for the removal of cationic dyes from water. Journal of Colloid and Interface Science. 281, 49 -55.

Bond, G. C. 1987. Heterogeneous Catalysis: Principles and Applications. Oxford University Press, New York, U.S.A.

Chuenchom, L. 2004. Adsorption of cadmium (II) and lead (II) ions on activated carbons obtained from bagasse and pericarp of rubber fruit. Master of Science Thesis in Physical Chemistry, Prince of Songkla University, Thailand.

Ferro-Garcy, M. A.; Rivera-Utrilla, J.; Bautista-Toledo, I. and Moreno-Castilla, C. 1998. Adsorption of Humic Substances on Activated Carbon from Aqueous Solutions and Their Effect on The Removal of Cr(III) Ions. Langmuir. 14, 1880-1886.

Hu, Z. and Vansant, E. F. 1995. A new composite adsorbent produced by chemical activation of elutrilithe with zinc chloride. Journal of Colloid and Interface Science. 176, 422

Jia, Y. F.; Steele, C. J.; Hayward, I. P. and Thomas. K. M. 1998. Mechanism of adsorption of gold and silver species on activated carbons. Carbon. 36, 1299-1308.

Jia, Y. F.; Xiao, B. and Thomas, K. M. 2002. Adsorption of metal ions on nitrogen surface functional groups in activated carbons. Langmuir. 18, 470-478.

Juang, R., Wu, F. and Tseng, R. 2002. Characterization and use of activated carbons prepared from bagasses for liquid-phase adsorption. Colloid. Surface: A. 201, 191-199.

Kadirvalu, K.; Faur-Brasquet, C. and Le Cloirec, P. 2000. Removal of Cu(II), Pb(II), and Ni(II) by Adsorption onto Activated Carbon Cloths. Langmuir. 16, 8404-8409.

Langmuir, I. 1918. Adsorption of gases on plane surfaces of glass, mica and platinum. Journal of the American Chemical Society. 40, 1361.

Lozano-Castello,D.; M.A. Lillo-Rodenas, D.; Cazorla-Amoros, and Linares-Solano, A. 2001. Preparation of activated carbons from Spanish anthracite I. Activation by KOH, Carbon. 39(5), 741-749.

Meikap, B.C., Thammu Naidu, J., Biswas, M.N. and Kaustubha, M. 2006. Removal of crystal violet from wastewater by activated carbons prepared from rice husk. Industrial and Engineering Chemistry Research, Eng. 45, 5165-5171.

McEnaney B. 2002. Handbook of porous solids; Schuth, F., Sing, K. S. W.; Weitkamp, J., Volume 3, Wiley-VCH Verlag GmbH, Weinheim, Germany.

Namasivayam, C., Muniasamy, N., Gayathri, K., Rani, M. and Renganathan, K. 1996. Removal of dyes from aqueous solution by cellulosic waste orange peel. Bio Research Technology. 57, 37.

Namasivayam, C. and Kadirvelu, K. 1999. Uptake of mercury (II) from wastewater by activated carbon from an unwanted agricultural solid by-product: coirpith. Carbon. 37, 79-84

Sirichote, O., Innajitara, W., Chuenchom, L., Chunchit, D. and Naweekan, K. 2002. Adsorption of iron (III) ions on activated carbons obtained from bagasse, pericarp of rubber fruit and coconut shell. Songklanakarin Journal of Science and Technology. 24, 235-242.

Sirichote, O., Innajitara, W., Chuenchom, L., Panumati, S., Chudecha, K., Vankhaew, P. and Choolert, V. 2008. Adsorption of phenol from diluted Aaqueous solutions by activated carbons obtained from bagasse, oil plam shell and pericarp of rubber fruit. Songklanakarin Journal of Science and Technology. 30(2), 185-189.

Strelko, V Jr. and Malik, D. J. 2002. Characterization and metal sorption properties of oxidized active carbon. Journal of Colloid and Interface Science. 250, 213-220.

Williams P. T. and A. R. Reed. 2004. High grade activated carbon matting derived from the chemical activation and pyrolysis of natural fibre textile waste. Journal of Analytical and Applied Pyrolysis. 71(2), 971-986.